water

MDPI

Article

The Influence of the Osmotic Potential on Evapotranspiration

Adil K. Salman [1,*], Wolfgang Durner [1], Mahyar Naseri [2] and Deep C. Joshi [3]

[1] Soil Science and Soil Physics Division, Institute of Geoecology, Technische Universität Braunschweig, Langer Kamp 19c, 38106 Braunschweig, Germany; w.durner@tu-braunschweig.de
[2] Thünen Institute of Agricultural Technology, Bundesallee 47, 38116 Braunschweig, Germany; mahyar.naseri@thuenen.de
[3] Research Institute for Post-Mining Landscapes (FIB) e.V., Brauhausweg 2, 03238 Finsterwalde, Germany; d.joshi@fib-ev.de
* Correspondence: a.al-salman@tu-braunschweig.de

Abstract: Climate change is expected to affect the quality of soil and water, resulting in a significant impact on soil water balance in various regions around the world. Soil water potential plays a significant role in influencing evapotranspiration (ET), which is a crucial component of the soil water balance. The matric potential and the osmotic potential are the main components of the soil water potential. The osmotic potential is particularly important in dry soils, salt-affected soils, coastal lands, or when low-quality water is utilized for irrigation. Despite its importance, the impact of osmotic potential on ET has not been well-studied compared to other factors. Therefore, we conducted a study to investigate the impact of osmotic potential on ET from small-scale lab lysimeters planted with grass and equipped with scales and data loggers connected to computers. To create different osmotic potential levels, we irrigated the lysimeters with two different water qualities: distilled water and 4.79 dS.m^{-1} NaCl solution. The lysimeters were kept in well-watered conditions, and daily ET was monitored. Our results indicate a strong correlation between osmotic potential and ET. After three months of applying the treatments, the lysimeters with lower osmotic potential had a 39% reduction in cumulative ET compared to those irrigated with distilled water. Moreover, the osmotic stress affected plant health, leading to a notable decrease in the leaf area index and exerting a significant influence on evapotranspiration partitioning components, including transpiration and evaporation.

Keywords: osmotic potential; soil salinity; evapotranspiration; water potential; water quality; salt-affected soils; irrigation requirement

Citation: Salman, A.K.; Durner, W.; Naseri, M.; Joshi, D.C. The Influence of the Osmotic Potential on Evapotranspiration. *Water* **2023**, *15*, 2031. https://doi.org/10.3390/w15112031

Academic Editors: Xiaobing Chen, Jingsong Yang, Jingwei Wu, Dongli She, Weifeng Chen, Yi Wang, Min Chen, Yuyi Li, Asad Sarwar Qureshi, Anshuman Singh and Edivan Rodrigues De Souza

Received: 20 April 2023
Revised: 19 May 2023
Accepted: 24 May 2023
Published: 26 May 2023

1. Introduction

Climate change is the most severe challenge that faces the whole world in the 21st century. Significant influences on global food security are expected [1], owing to the influences on water resources' quantity and quality, as well as on soil quality. Low precipitation, higher temperatures, and higher potential evapotranspiration, ETp, resulting in longer, harder, and more frequent droughts, are among the prospective events that result from the changes in weather patterns [2]. In parallel with the increase in temperature, soil and water salinity are likely to increase. Therefore, irrigation demand will significantly grow [3]. Sea-level rise (extremely saline water), along with expected more frequent droughts due to climate change, will affect the soils in coastal lands in addition to the expected influence in the arid and semi-arid regions. Recent studies have clarified that the impacts of climate change on water resources will also affect the wetter areas in central Europe [4]. In Germany, more and longer periods without precipitation are expected in the future [5]. In many studies, an increase in irrigation demand in different parts of the country is identified for the future [6–11]. As a result, improving water use efficiency through irrigation management and adopting advanced irrigation technology has become crucial and is considered one of the key adaption measures [9].

An accurate estimate of actual evapotranspiration (ETa) is crucial for optimizing irrigation scheduling and maximizing water use efficiency [12]. ETa is affected by various plant, meteorological, and soil factors. To determine the ETa rate for a specific crop, the grass reference evapotranspiration (ETo) must first be calculated. ETo is the rate of evapotranspiration from an extensive reference surface of green grass that has a uniform height of 0.12 m height and is actively growing, well-watered, and completely shading the ground [13]. This value can then be adjusted for specific crops using crop-specific factors. This value reduces to the actual ETa dependent on various factors, including soil dryness.

A soil-related key factor that influences ETa is the total soil water potential (Ψ). It consists of two main components: matric (Ψm) and osmotic potential (Ψo). The Ψo is a function of soluble salt content and it is influenced by the solute transport within the soil profile [14]. Unlike the other factors, the impact of Ψo on ET has not been sufficiently investigated in experimental studies. The rate of water flow from the soil to the plant root is controlled by the difference in the total water potential between the two ends of the pathway [15]. The same dynamic controls the water flow from the plant root to the plant leaf. Any change in Ψo affects the value of Ψ in the root zone and influences the transpiration rate of the plant. The effect might be amplified when soil becomes dry due to the concentration of soil solution. In dry or semi-arid conditions, salts accumulate in the root zone and at the soil surface, which produces very low values of the Ψ near the plant roots [16]. Electrical conductivity has been shown to have a significant impact on ETa [17–19], as well as on evaporation from bare soil surfaces [20–22].

In previous studies, researchers tried to model the response of water uptake by plants as a function of the electrical conductivity of soil saturated-paste extract (ECe), e.g., [17,23–25]. More recently, [26] modeled the ETa of tomato plants in response to ECe. However, the responses of ET to the in situ Ψo and specific ionic stresses are not clearly understood [26]. Therefore, the field irrigation scheduling is still based on retention curves which express water content just as function of the matric potential and disregard Ψo. Moreover, the influences of Ψo on ET are also neglected in most of the indirect methods for ET estimation, specifically micrometeorological methods, which are widely used. This oversight can lead to inaccurate irrigation scheduling and reduced irrigation efficiency. To address this issue, researchers utilizing the FAO56 crop water requirements method [13] have recommended adjusting the crop coefficient factor (Kc) to account for the stress coefficient (Ks) when salinity affects the plants [27,28]. However, the FAO56 approach for computing Ks for saline stress needs to be validated with a soil water balance [29].

The influence of osmotic potential on the soil water balance, including evapotranspiration, is qualitatively widely recognized, especially in areas affected by salt. However, the actual extent of its impact on evapotranspiration and its two constituents, namely, evaporation and transpiration, remains poorly understood, partly because experimental data on this are scarce. To address this knowledge gap, we conducted a laboratory study using small-scale lysimeters planted with grass and exposed to various osmotic conditions resulting from irrigation with varying water qualities. Our hypothesis was that osmotic potential in the bulk soil significantly affects the soil water balance, and our goal was to elucidate and quantify this influence, including its effects on evapotranspiration and its two constituents.

2. Materials and Methods

2.1. Experimental Setup

To accomplish our objective, we conducted a laboratory experiment using four small lysimeters that were equipped with scales and data loggers and planted with grass. The experiment involved two different irrigation water quality treatments, each replicated twice. The lysimeters, which were constructed from PVC cylinders with an inner diameter of 230 mm, were packed to a height of 200 mm and had a soil volume of 8.3 L. We filled each with 11.8 kg of air-dry sandy loam soil material. Table 1 shows some of the soil properties. The lysimeters were positioned on a workbench behind windows located on the west side

of a laboratory at TU Braunschweig, Germany, where they were exposed to natural sunlight (refer to Figure 1). The experiments took place for about five months including about three months for data collection, from September until end of November, 2020.

Table 1. Basic soil properties.

Sand	Silt	Clay	EC (1:1)	Bulk Density
0.65 kg kg^{-1}	0.29 kg kg^{-1}	0.06 kg kg^{-1}	0.59 dS m^{-1}	1.43 g cm^{-3}

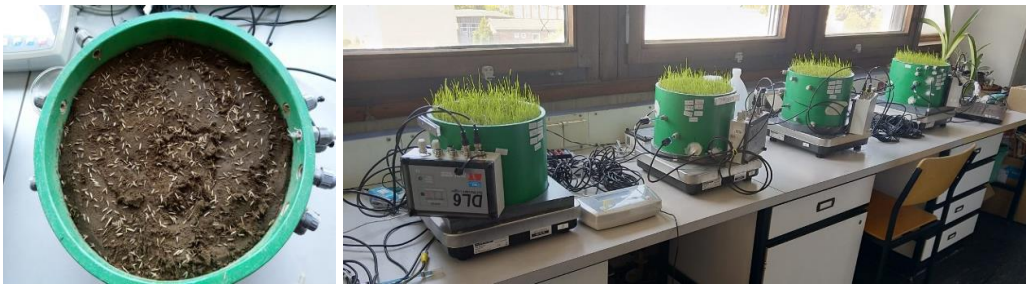

Figure 1. Experimental setup. (**Left**): Moist soil with the grass seeds. (**Right**): Four mini-lysimeters with DL6 data loggers mounted on scales after 18 days of initial growth.

The lysimeters were placed on weighing balances (DS 36K0.2, Kern and Sohn GmbH, Balingen, Germany) and connected to DL6 data loggers (METER Group Inc., Pullman, WA, USA). The hydraulic properties of the material have been determined at soil samples of 250 cm^3 that were packed to the same bulk density. We used the simplified evaporation method with the HYPROP (Hydraulic Property Analyzer, METER Group GmbH, Munich, Germany) system to obtain the retention and conductivity data and to fit parametric models to the data (Figure 2). The electrical conductivity of 1:1 (weighing ratio) dry-soil:water extracts was measured using an electrical conductivity meter with measurement correction to 20 °C.

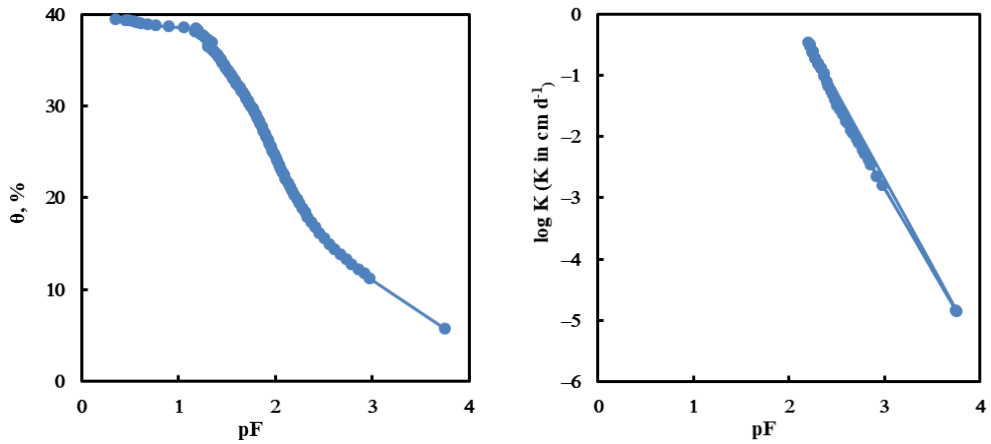

Figure 2. Retention curve and hydraulic conductivity curve of the material used in the small lysimeters. pF is defined by $\mathrm{pF} = \log 10(-h)$, where h is the matric potential expressed as pressure head in cm.

2.2. Initial Conditions

The lysimeters were packed in air-dry conditions, and the surface of the lysimeters was irrigated with distilled water until the moisture content reached the proper level (θ = 20%) for seed germination. Then, the lysimeters were planted with grass seeds (Lolium perenne). Each lysimeter received 1.3 g of seeds, which was evenly distributed on the soil surface (Figure 1, left). After seed germination, the lysimeters were manually irrigated

with distilled water in all treatments. Irrigation occurred when the mean volumetric water content decreased by 5%. When the plants reached a height of 12 cm, all lysimeters were harvested and the plant leaves were weighed to verify that all lysimeters had the same plant density. Thereafter, the grass continued to grow and when the plant height reached 12 cm, the irrigation treatments were applied.

2.3. Irrigation Treatments

The experiment consisted of two irrigation water quality treatments, each in two replicates. Two lysimeters were irrigated with distilled water (EC = 0 dS m^{-1}), whereas the other two were irrigated with a 2560 mg L^{-1} NaCl solution (EC = 4.79 dS m^{-1} at 20 °C). The osmotic potential of the pure saline solution was −1747 hPa. The use of distilled water is, of course, unusual in normal irrigation practice, but in this experiment our goal was not changing the total electrolyte content in the control treatments.

The plants were grown in well-watered conditions during the experiment, i.e., the volumetric water content of all treatments was kept between 15 and 20%. When the mean moisture content approached the lower threshold, irrigation was applied to increase the volumetric water content again to 20%, controlled by the lysimeter's weight. Table 2 shows the irrigation scheduling for the experiment. Plant height was also maintained at 12 cm during the experiment by cutting the grass three times a month.

Table 2. Irrigation scheduling.

Date	Distilled Water Irrigation, mm	Saline Water Irrigation, mm
7 September 2020	5.4	4.3
10 September 2020	11.3	8.1
16 September 2020	9.8	8.6
20 September 2020	10.9	8.7
23 September 2020	9.2	7.2
28 September 2020	11.2	7.4
2 October 2020	8.0	0.0
5 October 2020	0.0	9.3
9 October 2020	13.9	0.0
12 October 2020	0.0	8.4
14 October 2020	11.2	0.0
19 October 2020	9.7	8.2
23 October 2020	7.55	0.0
29 October 2020	9.6	8.8
5 November 2020	10.8	0.0
9 November 2020	8.9	9.6
16 November 2020	13.6	0.0
20 November 2020	0.0	9.2
23 November 2020	13.7	0.0
27 November 2020	9.7	0.0
Total irrigation, mm	174.5	97.9
Number of irrigation events	17	12

The changes in moisture, bulk electrical conductivity, and matric potential for each lysimeter were monitored. The evolution in osmotic potential in each lysimeter was calculated using Equations (2) and (3) considering the changes in soil moisture and bulk electrical conductivity. Daily and accumulated evapotranspiration were calculated based on the weighing balances data. The relationship between the evolution of osmotic potential and the daily evapotranspiration rate has been obtained. At the end of the experiment, when the soil became air-dry, samples were collected from three different depths (0–7, 7–14, and 14–20 cm) in each lysimeter to estimate the electrical conductivity and the spatial salt distribution.

2.4. Calculation of Osmotic Potential

Ψo can be estimated in soil solution using the Van't Hoff equation if both the concentration of solute and the ionic composition are known:

$$\Psi o = -CiRT \quad (1)$$

where C (Mol L^{-1}) is the molar concentration of the solutes, i (-) is the osmotic coefficient, R (8.31 J K^{-1} mol^{-1}) is the gas constant, and T (K) is the absolute temperature. However, the soil solution contains different salts; therefore, the use of the Van't Hoff equation requires knowledge of the chemical composition of the soil solution.

Alternatively, Ψo (atm) can be estimated from ECe (dS m^{-1}), using the U.S. Salinity Laboratory Staff model [30]:

$$\Psi o = -0.36\ ECe \quad (2)$$

In this work, we apply this empirical Equation (2), and express Ψo in units of hPa. The removal of water from the system will increase the salinity in the soil. We calculate the temporal evolution of the Ψo in the lysimeter in response to different volumetric water contents (θ) by the simple relationship given by Campbell [31]:

$$\Psi o\ (\theta) = \Psi o\ (\theta s)\frac{\theta s}{\theta} \quad (3)$$

where θs is the volumetric water content at saturation and θ is the reduced water content due to evapotranspiration. To ensure the representativeness of our osmotic potential estimations, we calculated the average value of Ψo for the entire volume of the lysimeter, under the assumption that the lysimeter's dimensions provided an adequate representation of the grass root-zone. Hereby, we assume that absorbed ions by the plant root are neglected, and, furthermore, we neglect the local spatial variability of θ and C due to root water uptake and evaporation.

2.5. ET Partitioning

For partitioning the two components of evapotranspiration, we applied the following procedure: We estimated the ground coverage (GC) fraction from pictures collected on the first day after applying the treatments, on day 20 when the influence of saline solution on plant health was firstly observed, and on day 86, which was the last day of the experiment. The images were processed in MATLAB using the CANOPEO tool. This tool was developed at Oklahoma State University and can be freely downloaded (https://canopeoapp.com (accessed on 3 February 2023)) to be integrated with MATLAB; it is capable of accurately estimating the GC by processing images or videos [32,33]. Figure 3 shows the original and processed images for GC estimation.

Leaf area index, LAI (m^2 m^{-2}) is calculated from the GC (%) values using the linear model suggested by [34] for grass as follows:

$$LAI = 0.0299 \times GC \quad (4)$$

The evaporation (E) part (mm d^{-1}) is calculated using a model related the ET (mm d^{-1}) and LAI values [35], and the transpiration (T) part is calculated as complementary term by subtracting E from ET:

$$E = \exp(-0.6\ LAI)\ ET \quad (5)$$

$$T = ET - E \quad (6)$$

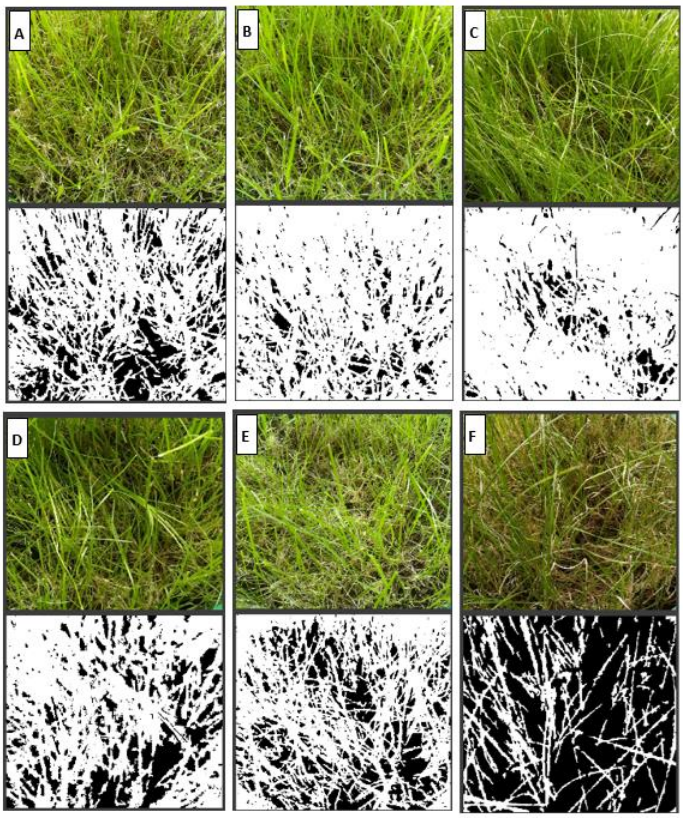

Figure 3. Original and processed images used in GC estimation. The images are labeled as (**A**–**C**) for the distilled water treatment at days 1, 20, and 86 after treatment application, and (**D**–**F**) for the saline water treatment at days 1, 20, and 86 after treatment application.

3. Results and Discussion

Figure 4 shows the temporal evolution in the Ψo values calculated by Equation (3) for both treatments during the experiment. The small variability between the two replicates indicates that the measured values are representative for the system. The trend of the Ψo values for the lysimeters that were irrigated with distilled water (blue curves) appears to be stable throughout the study period due to the stability of the total amount of soluble salts in the soil. However, a very slight change has been observed due to the drying–wetting cycles, which lead to a change in the concentration of the soil solution.

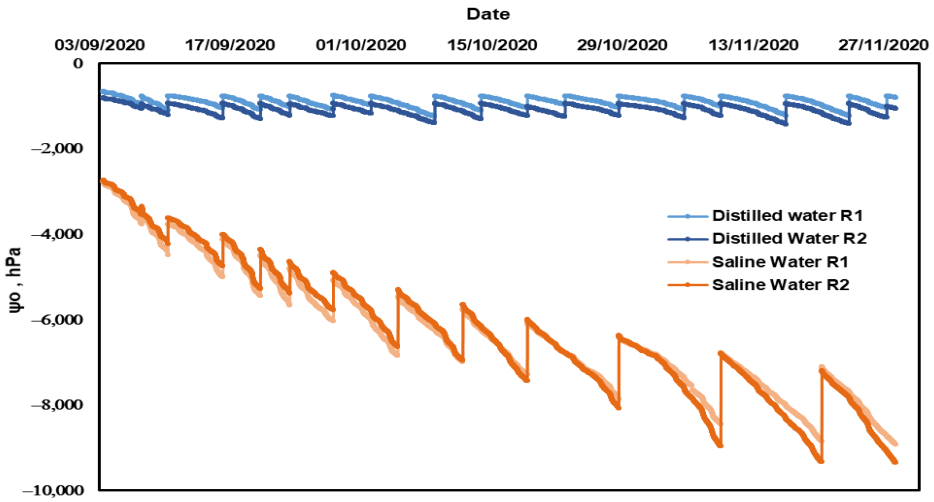

Figure 4. Evolution in Ψo values for the lysimeters during the experiment.

The evolution of Ψo for the saline water treatments is depicted by the orange data. The trend shows an almost linear decrease in the calculated mean osmotic potential due to the irrigation with saline water during the study period, caused by the added salt by each irrigation event. An instant increase in the Ψo value is observed directly after each irrigation event in response to the dilution process for the soil solution. After that, the Ψo values start to decrease following the drought process that concentrates the soil solution. Due to the higher salinity level in the saline treatment, the influence of drying–wetting cycles on the Ψo are far more pronounced compared to the distilled water treatment, and the impact increases after each irrigation event due to the ongoing salt accumulation.

Figure 5 shows the average daily evapotranspiration for the treatments studied. Evapotranspiration rates varied from day to day due to meteorological conditions and decreased in both treatments. This general trend followed the change in environmental conditions with shorter daylight hours as the experiments began in early September and continued through late November. The reduction in daily ET in the saltwater treatments was prevalent already from the beginning, but became more pronounced over time. The reduction started at about 10% and reached 55% after three months of applying the treatments.

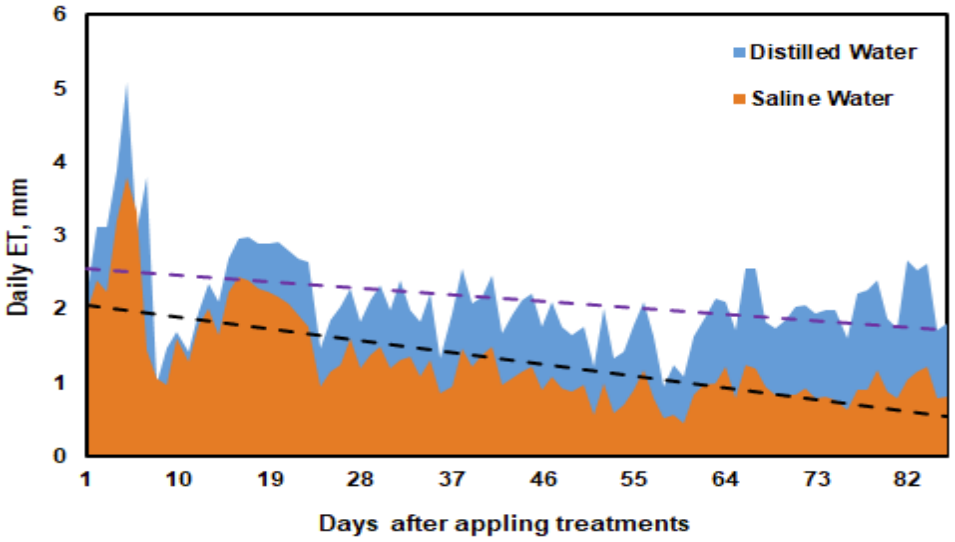

Figure 5. Average daily evapotranspiration values for the treatments during the experiment.

Since soil moisture was kept high enough to meet the ETo requirement, the relative reduction in the salt treatment is entirely due to the effect of salt on both evaporation and transpiration. The change in soluble salt content leads to a decrease in evaporation rate due to the reduction in water vapor pressure [36]. On the other hand, the transpiration rate decreased due to the effects on the gradient of soil water potential between soil and plant root, which controls the flow of water through the soil–plant system [15,16]. With ongoing time, this was superimposed by a deterioration in plant health, which was observed in the salt treatment from about 20 days after treatment, as shown in Figure 6.

Figure 7 shows the effect of the experimental treatments on cumulative evapotranspiration. At the end of the experiment, accumulated evapotranspiration reached 112 mm in the saline treatment, while it was 184 mm in the treatments irrigated with distilled water. The reduction in cumulative evapotranspiration was 39% during the experimental period. It is noteworthy that irrigation with saline water resulted in a reduction in the number of irrigation events required, with a recorded frequency of 12 events, compared to the 17 events observed in the distilled water treatment (Table 2).

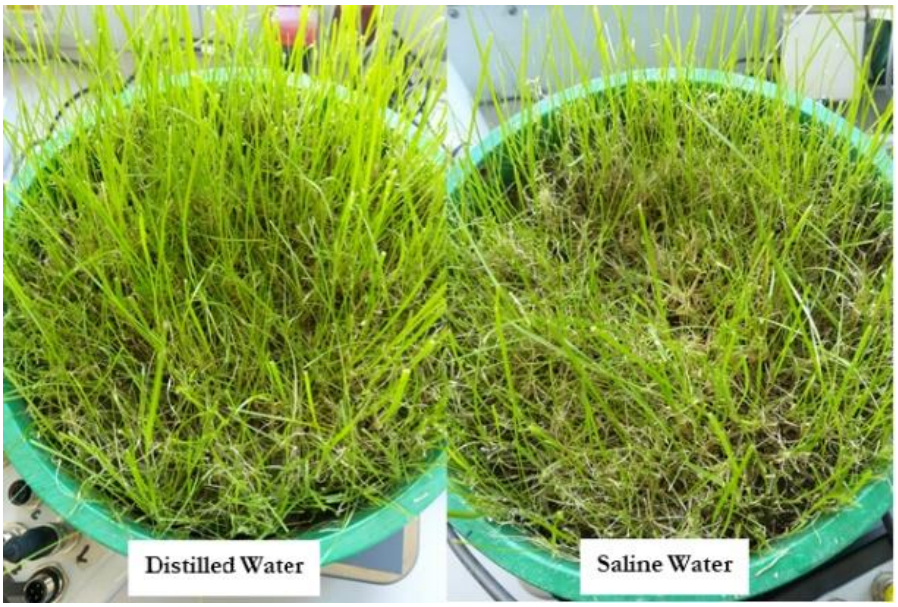

Figure 6. Reduced plant health of the saline irrigated variant, 20 days after applying the treatments.

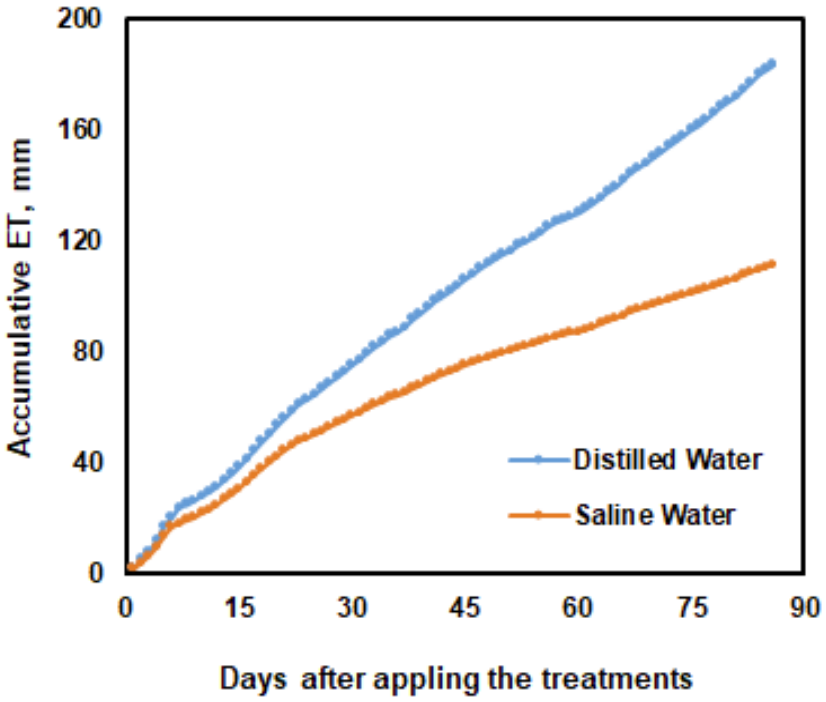

Figure 7. Cumulative evapotranspiration in response to the experimental treatments.

The underlying cause can be attributed to the influence of osmotic stress, which affects plant water uptake by influencing the hydraulic gradient in the root zone. As a consequence, this influence leads to a reduction in water loss through transpiration from plant leaves [15,16]. Additionally, the accumulation of soluble salts affects water vapor pressure, resulting in a reduction in evaporation from the soil surface [20]. These combined effects caused a reduced amount of cumulative evapotranspiration for osmotic stress-treated plants, and, accordingly, a reduced amount and frequency of required irrigation events.

The partitioning of ET into its components, E and T, is illustrated in Figure 8. The figure displays the response of E and T to Ψo on the first day after treatment application, on day 20, when the impact on plant health was first observed, and on day 86, which was the final day of the experiment. The data show a roughly comparable immediate response from

both ET components on the first day after treatments. The values for E and T for the saline water treatment on day 1 were 0.54 mm d^{-1} and 1.44 mm d^{-1}, respectively, while they were 0.60 mm d^{-1} and 1.58 mm d^{-1} for distilled water treatment. Thus, both components were reduced by roughly 10%.

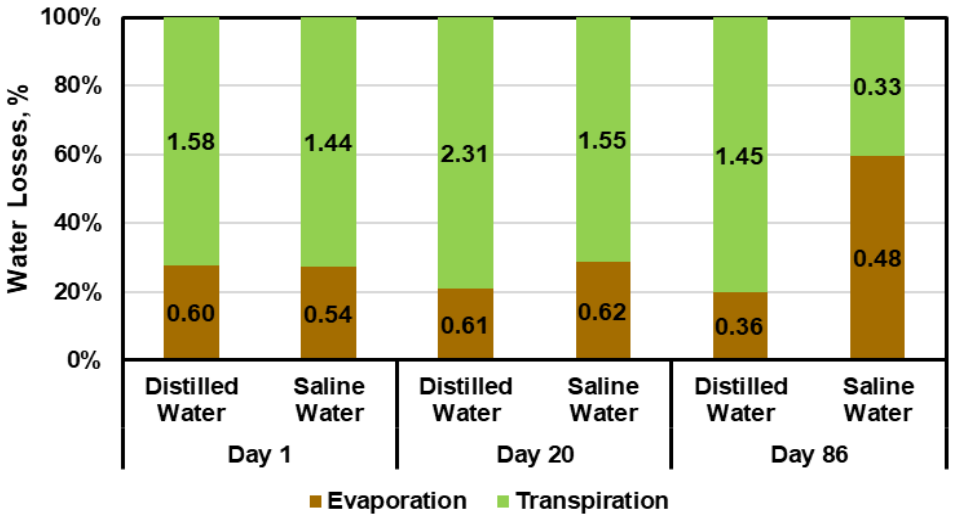

Figure 8. Partitioning of ET.

In the further course of the experiment, the increasing impact of saline solution on plant health is reflected in the reduction in GC and LAI, as presented in Table 3 for three key dates. The relative decrease in the transpiration component for the saline water treatment became stronger with time. On day 20, the values for E and T for the saline water treatment were 0.62 mm d^{-1} and 1.55 mm d^{-1}, while they were 0.61 mm d^{-1} and 2.31 mm d^{-1} for the distilled water treatment. In the further course of the experiment, the evaporation rate for the saline water treatment was, interestingly, slightly higher than that of the distilled water treatment, which can be attributed to the decrease in GC, which, in turn, increased the available surface area of the soil for evaporation. On day 86, this effect was most pronounced due to the substantial reduction in GC and LAI (Table 3) for the saline solution treatment, which showed an evaporation value of 0.48 mm d^{-1} compared to the distilled water treatment with 0.36 mm d^{-1}. In contrast, transpiration was lowered in the saline variant down to 0.33 mm d^{-1} compared to the distilled water treatment with 1.45 mm d^{-1}.

Table 3. GC, LAI, and partitioning of ET components.

Treatment	Day	GC (%)	LAI (m^2 m^{-2})	ET (mm d^{-1})	E (mm d^{-1})	T (mm d^{-1})
Distilled water	1	71.8	2.15	2.19	0.60	1.58
	20	87.5	2.62	2.91	0.61	2.31
	86	90.6	2.71	1.81	0.36	1.45
Saline water	1	72.5	2.17	1.98	0.54	1.44
	20	69.6	2.08	2.18	0.62	1.55
	86	29.0	0.87	0.81	0.48	0.33

The reduction in ET and its components in the saline solution treatment is due to the two-phase growth response to salt stress [37], which includes an osmotic process caused by salt accumulation in the root zone, reducing osmotic potential and plant growth, and an ion-specific process leading to further reduction in plant growth due to soil nutrient balance and plant cellular processes.

The relationship between Ψo and ETa is presented in Figure 9. ETa in this figure refers to the daily evapotranspiration from the lysimeters that were irrigated with saline solution, while the ETo refers to the evapotranspiration from the lysimeters that were irrigated

with distilled water. We assume that the evapotranspiration values for the distilled water treatment can serve as a reference for comparison. The data in Figure 9 show a strong and roughly linear relationship between ETa/ETo and Ψo. The decreasing Ψo in the root zone causes a significant reduction in the daily evapotranspiration. At the lowest values of Ψo, when it reached about −9000 hPa, the ETa/ETo ratio was about 0.4, i.e., the reduction in the daily evapotranspiration reached 60%.

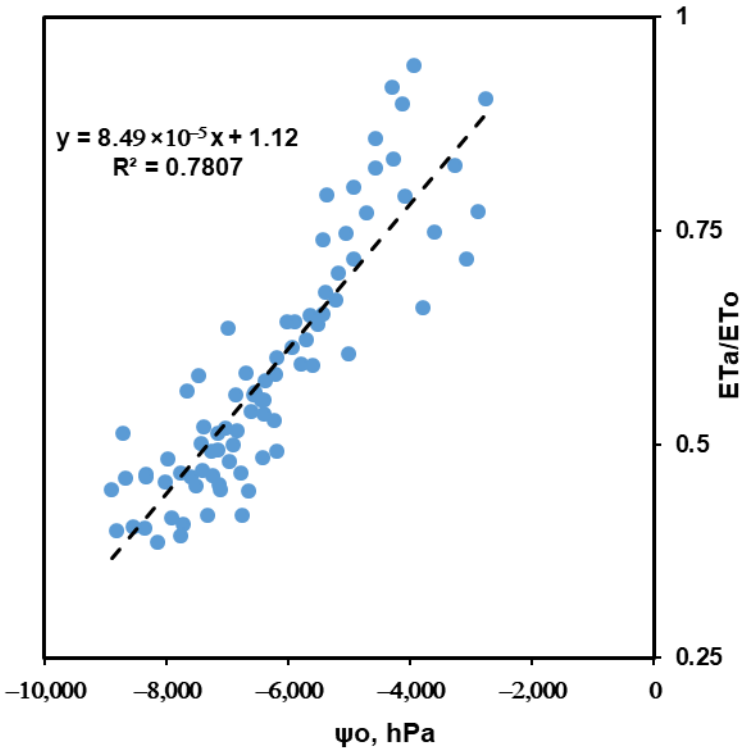

Figure 9. The influence of Ψo on the ETa/ETo ratio.

We attribute this reduction to two factors. The first factor is the water potential gradient, which controls the water flow through the soil–root–leaf–atmosphere system, as well as the water flow directly from the soil to the atmosphere. Water potential directly controls the function of leaves, roots, and microbes, and gradients in water potential drive water flows throughout the soil–plant–atmosphere continuum [38]. The transpiration rate from plant leaves is determined by the water potential gradient between the root surfaces and the leaves, divided by the plant resistance factor. When the water potential decreases, the hydraulic gradient is reduced and the plant resistance factor increases, leading to a reduction in the transpiration rate [15].

The second factor is the plant-health factor, which refers to the effect on plant biological activities and the nutrient balance. The impact of the second factor leads to a reduction in LAI and thus affects transpiration and, complementarily, increases relative evaporation. The influence on plant health is strongly correlated to the type of the prevalent ions in the soil solution and their concentration, as well as to the plant-specific parameters such as plant type, growth stage, species and variety [37].

The simple linear relation in Figure 9 allows the calculation of the reduction in ET in response to the decrease in the osmotic potential in the root zone. Mathematically, and based on the collected data, the evapotranspiration under osmotic influence ($ET_{\Psi o}$) can be expressed as:

$$ET_{\Psi o} = f \times ET_0 \quad (7)$$

where

$$f = \begin{cases} 5.8 \times 10^{-5} \times \Psi o \text{ for } \Psi o < \Psi o^* \\ 1 \text{ for } \Psi o \geq \Psi o^* \end{cases} \quad (8)$$

In Equation (8), Ψo* is the threshold point at about −1400 hPa, up to which there is no significant impact from the Ψo with respect to the reference. Equation (8) shows that beyond this threshold, a 1000 hPa decrease in Ψo causes an 8.5% decrease in $ET_{\Psi o}/ET_0$. A 100% decrease in ET would be reached if the osmotic potential drops to −13,200 hPa, which is about 11,800 hPa from the threshold. This value is close to that of [39], who found that Perenne grass can turn yellow within two weeks when the electrical conductivity of the growing medium (Hoagland solution) reaches 24 dS m^{-1}, corresponding to an osmotic potential of about −8800 hPa. Equation (8) is based on empirical data of our experiment and we expect that it may depend on the plant species and the dominating ion type in the soil solution. The model should be tested in real-field conditions under wide range of soil salinity cases.

Figure 10 finally shows the electrical conductivity of the 1:1 soil:water extracts for the studied treatments, obtained in three depth layers after the end of the experiment. The results indicate a strong salt accumulation due to the irrigation with saline solution, but also a relative accumulation of native salt in the soil in the control. The electrical conductivity of the top layer reached 8.2 dS m^{-1} for the saline water treatment, while it was 0.76 dS m^{-1} for the distilled water treatment. These results indicate that primarily due to evaporation, most of the soluble salts moved to the upper layer. For the distilled water treatment, the electrical conductivity for the top layer was 0.76 dS m^{-1}, while it was 0.12 and 0.09 dS m^{-1} for the middle and lower layers, respectively. In the case of the saline solution treatment, the electrical conductivity for the upper, middle, and lower layers was 8.20, 0.95, and 0.46 dS m^{-1} in succession. The illustration of the salinity distribution shows the importance of the soil water flow, whether the flow is within the soil profile or through the soil–atmosphere or soil–plant systems. This is particularly important in arid and semi-arid regions, salt-affected soils, coastal lands, and when low-quality water is used for irrigation. When the salts accumulate near the soil surface, they apply a driving force to the soil surface and affect the water flow. The accumulation of soluble salts on the soil surface results in an increase in hydraulic gradient by reducing the osmotic potential, thereby stimulating the movement of water from the soil body towards the surface. On the other hand, precipitation of salts on the soil surface reduces the flow of water from the soil to the atmosphere, due to the mulching effect of the precipitated salts on the soil surface.

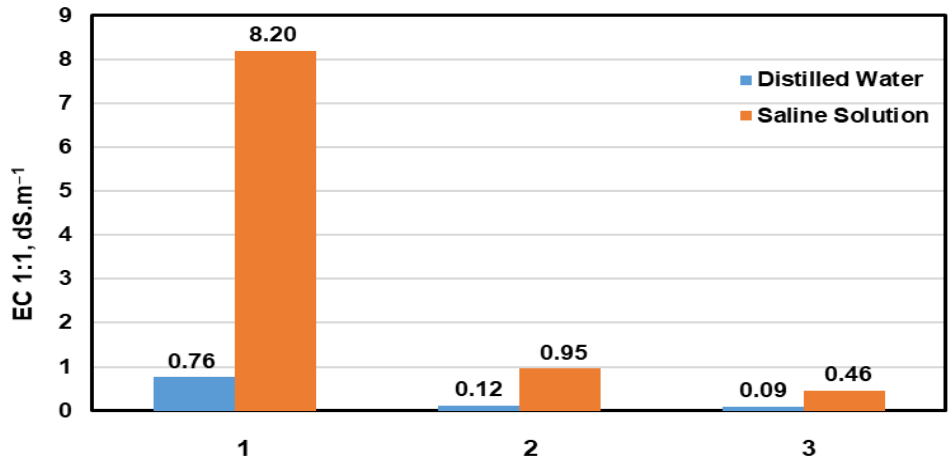

Figure 10. Electrical conductivity at the soil surface (1), mid layer (2), and lower layer (3).

4. Conclusions

In an experimental study, we investigated the impact of osmotic potential on evapotranspiration from small-scale laboratory lysimeters planted with grass. To achieve this, we used two different water quality levels for irrigation. The first level involved the use of distilled water for irrigation, which ensured a constant total salt content in the lysimeters during the experiment and maintained the mean osmotic potential at a stable level. In

contrast, the second treatment involved the use of a 4.79 dS m^{-1} NaCl solution for irrigation, which continuously decreased the osmotic potential throughout the study. We used average values in the lysimeters in this study to find a relationship between ET reduction and osmotic potential, because a detailed characterization of the spatiotemporal local distribution and evolution of osmotic potential in the root zone, including salt accumulation in the near rhizosphere, would be beyond the goal of this study, both in terms of measurement and practicality of the model.

Our results indicated a strong relationship between the mean osmotic potential in the system and the evapotranspiration. We observed a 10% reduction in daily evapotranspiration immediately after applying the treatments, with the reduction reaching approximately 55% at the end of the study. The cumulative evapotranspiration reduced by 39% over the three-month data collection period. These findings highlight the importance of considering osmotic potential in water balance studies, irrigation scheduling, and watershed management, particularly in regions with arid and semi-arid climates, salt-affected soils, coastal areas, and when using low-quality water, such as wastewater, for irrigation. However, large-scale field studies are needed to investigate the role of osmotic potential in evapotranspiration under more complex natural conditions and to consider different water and soil qualities and salinity compositions.

Author Contributions: A.K.S.: conceptualization, methodologies, experimental setup, data collection and analysis, writing—original draft preparation. W.D.: conceptualization, writing—review and editing. M.N.: experimental setup. D.C.J.: experimental setup. All authors have read and agreed to the published version of the manuscript.

Funding: The Alexander von Humboldt Foundation through the PSI funding program funded this research.

Data Availability Statement: The data for this study's findings are available from the corresponding author upon reasonable request.

Conflicts of Interest: The authors declare no conflict of interest.

References

1. FAO. *Climate Change and Food Security: Risks and Responses*; FAO: Rome, Italy, 2015; ISBN 978-92-5-108998-9. Available online: http://www.fao.org/3/i5188e/i5188e.pdf (accessed on 10 January 2023).
2. Corwin, D.L. Climate change impacts on soil salinity in agricultural areas. *Eur. J. Soil Sci.* **2021**, *72*, 842–862. [CrossRef]
3. Okur, B.; Orcen, N. Soil salinization and climate change. In *Climate Change and Soil Interactions*; Prasad, M.N.V., Pietrzykowski, M., Eds.; Elsevier: Amsterdam, The Netherlands, 2020; ISBN 978-0-12-818032-7. [CrossRef]
4. Riediger, J.; Breckling, B.; Nuske, R.S.; Schröder, W. Will climate change increase irrigation requirements in agriculture of Central Europe? A simulation study for Northern Germany. *Environ. Sci. Eur.* **2014**, *26*, 18. [CrossRef] [PubMed]
5. Schmidt, N.; Zinkernagel, J. Modelling evapotranspiration and water demand of vegetables induced by climate change for irrigation purposes. *Acta Hortic.* **2014**, *1038*, 287–294. [CrossRef]
6. Steidl, J.; Schuler, J.; Schubert, U.; Dietrich, O.; Zander, P. Expansion of an Existing Water Management Model for the Analysis of Opportunities and Impacts of Agricultural Irrigation under Climate Change Conditions. *Water* **2015**, *7*, 6351–6377. [CrossRef]
7. Kreins, P.; Henseler, M.; Anter, J.; Herrmann, F.; Wendland, F. Quantification of Climate Change Impact on Regional Agricultural Irrigation and Groundwater Demand. *Water Resour. Manag.* **2015**, *29*, 3585–3600. [CrossRef]
8. Herrmann, F.; Kunkel, R.; Ostermann, U.; Vereecken, H.; Wendland, F. Projected impact of climate change on irrigation needs and groundwater resources in the metropolitan area of Hamburg (Germany). *Environ. Earth Sci.* **2016**, *75*, 1104. [CrossRef]
9. Umweltbundesamt. 2019 Monitoring Report on the German Strategy for Adaptation to Climate Change. 2020. Available online: https://www.umweltbundesamt.de/sites/default/files/medien/421/publikationen/das_2019_monitoring_report_bf.pdf (accessed on 12 January 2023).
10. Nickel, S.; Schröder, W. Fuzzy modelling and mapping soil moisture for observed periods and climate scenarios. An alternative for dynamic modelling at the national and regional scale? *Ann. For. Sci.* **2017**, *74*, 71. [CrossRef]
11. Harsch, N.; Brandenburg, M.; Klemm, O. Large-scale lysimeter site st. Arnold, germany: Analysis of 40 years of precipitation, leachate and evapotranspiration. *Hydrol. Earth Syst. Sci.* **2009**, *13*, 305–317. [CrossRef]
12. Gu, Z.; Qi, Z.; Burghate, R.; Yuan, S.; Jiao, X.; Xu, J. Irrigation Scheduling Approaches and Applications: A Review. *J. Irrig. Drain. Eng.* **2020**, *146*, 04020007. [CrossRef]
13. Allen, R.G.; Pereira, L.S.; Raes, D.; Smith, M. *Crop Evapotranspiration-Guidelines for Computing Crop Water Requirements*; FAO Irrigation and Drainage Paper 56; FAO: Rome, Italy, 1998.

14. Hillel, D. *Environmental Soil Physics*; Academic Press: New York, NY, USA, 1998.
15. Hamza, M.A.; Aylmore, L.A.G. Soil solute concentration and water uptake by single lupin and radish plant roots (II. Driving forces and resistances). *Plant Soil* **1992**, *145*, 197–205. [CrossRef]
16. Hamza, M.A.; Aylmore, L.A.G. Soil solute concentration and water uptake by single lupin and radish plant roots (I. Water extraction and solute accumulation). *Plant Soil* **1992**, *145*, 187–196. [CrossRef]
17. Homaee, M.; Dirksen, C.; Feddes, R.A. Simulation of root water uptake: I. Non-uniform transient salinity using different macroscopic reduction functions. *Agric. Water Manag.* **2002**, *57*, 89–109. [CrossRef]
18. Ali, A.; Yang, H.; Shukla, M. Brackish groundwater and RO concentrate influence soil physical and thermal properties and pecan evapotranspiration. *Soil Sci. Soc. Am. J.* **2021**, *85*, 1519–1533. [CrossRef]
19. Salman, A.; Durner, W.; Joshi, D.C.; Naseri, M. The response of Evapotranspiration to osmotic potential in small-scale lab lysimeters. In Proceedings of the EGU General Assembly, Online, 19–30 April 2021. EGU21-3033. [CrossRef]
20. Shokri-Kuehni, S.M.S.; Vetter, T.; Webb, C.; Shokri, N. New insights into saline water evaporation from porous media: Complex interaction between evaporation rates, precipitation, and surface temperature. *Geophys. Res. Lett.* **2017**, *44*, 5504–5510. [CrossRef]
21. Salman, A.; Joshi, D.; Naseri, M.; Durner, W. Evaporation from porous media as influenced by osmotic potential. In Proceedings of the EGU General Assembly, Online, 4–8 May 2020. EGU2020-9693. [CrossRef]
22. Li, X.; Shi, F. Effects of evolving salt precipitation on the evaporation and temperature of sandy soil with a fixed groundwater table. *Vadose Zone J.* **2021**, *20*, 3. [CrossRef]
23. Maas, E.V.; Hoffman, G.J. Crop salt tolerance-current assessment. *J. Irrig. Drain. Div.* **1977**, *103*, 115–134. [CrossRef]
24. Van Genuchten, M.T.; Hoffman, G.J. Analysis of crop production. In *Soil Salinity under Irrigation*; Shainberg, I., Shalhevet, J., Eds.; Springer: Berlin/Heidelberg, Germany, 1984; pp. 258–271.
25. Dirksen, C.; Kool, J.B.; Koorevaar, P.; Van Genuchten, M.T. HYSWASORsimulation model of hysteretic water and solute transport in the root zone. In *Water Flow and Solute Transport in Soils*; Russo, D., Dagan, G., Eds.; Springer: New York, NY, USA, 1993; pp. 99–122.
26. Yang, H.; Du, T.; Mao, X.; Shukla, M.K. Modeling tomato evapotranspiration and yield responses to salinity using different macroscopic reduction functions. *Vadose Zone J.* **2020**, *19*, e20074. [CrossRef]
27. Pereira, L.S.; Paredes, P.; Jovanovic, N. Soil water balance models for determining crop water and irrigation requirements and irrigation scheduling focusing on the FAO56 method and the dual Kc approach. *Agric. Water Manag.* **2020**, *24*, 106357. [CrossRef]
28. Pereira, L.S.; Paredes, P.; Hunsaker, D.; López-Urrea, R.; Jovanovic, N. Updates and advances to the FAO56 crop water requirements method. *Agric. Water Manag.* **2021**, *248*, 106697. [CrossRef]
29. Minhas, P.S.; Tiago, B.R.; Ben-Gal, A.; Pereira, L.S. Coping with salinity in irrigated agriculture: Crop evapotranspiration and water management issues. *Agric. Water Manag.* **2020**, *227*, 105832. [CrossRef]
30. U.S. Salinity Laboratory Staff. Diagnosis and improvement of saline and alkali soils. In *U.S. Department of Agriculture Handbook 60*; U.S. Salinity Laboratory: Washington, DC, USA, 1954. [CrossRef]
31. Campbell, G.S. *Soil Physics with BASIC*; Elsevier: Amsterdam, Switzerland, 1985.
32. Patrignani, A.; Ochsner, T.E. Canopeo: A powerful new tool for measuring fractional green canopy cover. *Agron. J.* **2015**, *107*, 2312–2320. [CrossRef]
33. González-Esquiva, J.M.; Oates, M.J.; García-Mateos, G.; Moros-Valle, B.; Molina-Martínez, J.M.; Ruiz-Canales, A. Development of a visual monitoring system for water balance estimation of horticultural crops using low cost cameras. *Comput. Electron. Agric.* **2017**, *141*, 15–26. [CrossRef]
34. Ramírez-García, J.; Almendros, P.; Quemada, M. Ground cover and leaf area index relationship in a grass, legume and crucifer crop. *Plant Soil Environ.* **2012**, *58*, 385–390. [CrossRef]
35. Belmans, C.; Wesseling, J.G.; Feddes, R.A. Simulation model of the water balance of a cropped soil: SWATRE. *J. Hydrol.* **1983**, *63*, 271–286. [CrossRef]
36. Al-Shammiri, M. Evaporation rate as a function of water salinity. *Desalination* **2002**, *150*, 189–203. [CrossRef]
37. Munns, R.; Tester, M. Mechanisms of Salinity Tolerance. *Annu. Rev. Plant Biol.* **2008**, *59*, 651–681. [CrossRef]
38. Novick, K.A.; Ficklin, D.L.; Baldocchi, D.; Davis, K.J.; Ghezzehei, T.A.; Konings, A.G.; MacBean, N.; Raoult, N.; Scott, R.L.; Shi, Y.; et al. Confronting the water potential information gap. *Nat. Geosci.* **2022**, *15*, 158–164. [CrossRef]
39. Friell, J.; Watkins, E. Review of Cool-Season Turfgrasses for Salt-Affected Roadsides in Cold Climates. *Crops Sci.* **2020**, *61*, 2893–2915. [CrossRef]